Suck, D., Lahm, A., & Oefner, C. (1988) *Nature (London) 332*, 464–468.
Viola, R. E. (1991) *Bioorg. Chem. 19*, 190–224.
Wertman, K. F., Wyman, A. R., & Botstein, D. (1986) *Gene 49*, 253–262.
Wilke, K., Rauhut, E., Noyer-Weidner, M., Lauster, R., Pawlek, B., Behrens, B., & Trautner, T. A. (1988) *EMBO J. 7*, 2601–2609.
Wu, J. C., & Santi, D. V. (1987) *J. Biol. Chem. 262*, 4778–4786.
Wu, J. C., & Santi, D. V. (1988) *Nucleic Acids Res. 16*, 703–717.
Zhou, X.-X., & Chattopadhyaya, J. (1986) *Tetrahedron 42*, 5149–5156.

Carbon-13 Nuclear Magnetic Resonance Spectroscopy of Lipids: Differential Line Broadening Due to Cross-Correlation Effects as a Probe of Membrane Structure†

Eric Oldfield,* Foluso Adebodun, John Chung, Bernard Montez, Ki Deok Park, Hong-biao Le, and Brian Phillips
School of Chemical Sciences, University of Illinois, 505 South Mathews Avenue, Urbana, Illinois 61801
Received August 27, 1991; Revised Manuscript Received October 2, 1991

ABSTRACT: We have obtained proton-coupled carbon-13 nuclear magnetic resonance (NMR) spectra of a variety of lipid–water and lipid–drug–water systems, at 11.7 T, as a function of temperature, using the "magic-angle" sample-spinning (MAS) NMR technique. The resulting spectra show a wide range of line shapes, due to interferences between dipole–dipole and dipole–chemical shielding anisotropy interactions. The differential line-broadening effects observed are particularly large for aromatic and olefinic (sp^2) carbon atom sites. Coupled spectra of the tricyclic antidepressants desipramine and imipramine, in 1,2-dimyristoyl-*sn*-glycero-3-phosphocholine–water mesophases, show well-resolved doublets having different line shapes for each of the four aromatic methine groups, due to selective averaging of the four C–H dipolar interactions due to rapid motion about the director (or drug C_2) axis. ^2H NMR spectra of [2,4,6,8-$^2H_4$]desipramine (and imipramine) in the same 1,2-dimyristoyl-*sn*-glycero-3-phosphocholine–water mesophase exhibit quadrupole splittings of ~0–2 and ~20 kHz, indicating an approximate magic-angle orientation of the C2–^2H(^1H) and C8–^2H(^1H) vectors with respect to an axis of motional averaging, in accord with the ^{13}C NMR results. Selective deuteration of imipramine confirms these ideas. Spectra of digalactosyl diglyceride [primarily 1,2-di[(9*Z*,12*Z*,15*Z*)-octadeca-9,12,15-trienoyl]-3-(α-D-galactopyranosyl-1–6-β-D-galactopyranosyl)-*sn*-glycerol]–H_2O (in the L_α phase) show a large differential line broadening for C9 but a reduced effect for C10, consistent with the results of ^2H NMR of specifically ^2H-labeled phospholipids [Seelig, J., & Waespe-Šarac̆evič, N. (1978) *Biochemistry 17*, 3310–3315]. Thus, both desipramine and imipramine and the glycolipid show magic-angle orientation effects which reduce the amount of differential line broadening observed with other C–H vector orientations. In monogalactosyl diglyceride [primarily 1,2-di[(9*Z*,12*Z*,15*Z*)-octadeca-9,12,15-trienoyl]-3-β-D-galactopyranosyl-*sn*-glycerol]–H_2O (in the H_{II} phase), similar differential line-broadening effects are found for C9,10; C12,13, and C15,16, upon cooling. The resonances of C9 and C10 broaden before those of C12,13, which in turn broaden before those of C15,16. C10 is narrower than C9, and has less differential broadening, consistent with a magic-angle orientation. Computer simulations of the low-temperature spectra of monogalactosyl diglyceride (at −30 °C) using chemical shift and intensity values from the high-temperature spectra permit determination of individual component line widths, even in spectra showing limited overall resolution. Each of the six olefinic carbons (in the mainly linolenoyl chains) exhibits differential line broadening. The good qualitative agreement between ^{13}C and ^2H NMR results suggests that useful orientational (^2H NMR like) information can be deduced from natural-abundance ^{13}C NMR spectra of a variety of mobile solids.

Nuclear magnetic resonance (NMR) spectroscopy has been used for a number of years to study lipid membrane structure, using a variety of natural-abundance as well as isotopic-labeling techniques (Veksli et al., 1969; Seelig, 1977; Rothgeb & Oldfield, 1981; Sefcik et al., 1983; Xu & Cafiso, 1986). Deuterium NMR has been particularly successful (Seelig, 1977; Renou et al., 1989; Vist & Davis, 1990), and more recently ^1H and ^{13}C "magic-angle" sample-spinning (MAS) methods have shown some promise (Forbes et al., 1988). Ideally, a membrane lipid probe would be capable of giving rate information, as well as order parameter information, without use of isotopic enrichment, and at high resolution. At present, however, spectroscopists in general use either low-resolution (^2H) NMR of isotopically labeled lipids or ^1H or ^{13}C MAS, the latter usually taken under conditions of full ^1H decoupling (Sefcik et al., 1983; Forbes et al., 1988). In this paper, we show that *coupled* ^{13}C MAS NMR appears to have potential for combining orientational as well as the more conventional dynamic structural information about the lipid components of membranes that is qualitatively (at present) similar to that deduced by ^2H NMR but does not involve isotopic labeling.

The method used involves conventional magic-angle sample spinning of lipid systems, but without cross-polarization (Pines et al., 1972) or proton decoupling. "*J*-coupled" spectra are obtained, and in situations where the chemical shift anisotropies are relatively large, interference effects between the

† This work was supported by the U.S. Public Health Service (Grant GM-40426).

0006-2960/91/0430-11025$02.50/0

C–H dipolar and ^{13}C chemical shift anisotropy (as well as dipole–dipole interferences, in some cases) cause differential line broadening of the individual components of a *J*-coupled multiplet. This type of interference effect is not new: it was first observed and explained in electron spin resonance (McConnell, 1956) and has had a number of applications in both liquid-state (Shimizu, 1964; Mackor & MacLean, 1966; Farrar & Quintero-Arcaya, 1987) and solid-state NMR (Harris et al., 1985; Hartzell et al., 1989). However, the solid-state NMR applications have been few.

What we have found is that the observation of differential line broadening (DLB) is very widespread and is exhibited by, e.g., glycerol at low temperature (Oldfield et al., 1991) and smectic, nematic, cholesteric, hexagonal, and cubic liquid crystals, as well as elastomers, e.g., poly(*cis*-butadiene) and poly(*cis*-isoprene) (Oldfield et al., 1991). In this paper, we discuss ^{13}C MAS DLB results for two tricyclic antidepressant drugs in a lipid–water system, as well as results on the L_α phase of the glycolipid digalactosyl diglyceride and the H_{II} phase of monogalactosyl diglyceride, emphasizing, where appropriate, similarities between the natural-abundance DLB MAS approach and results obtained by using ^2H NMR of labeled samples.

Experimental Procedures

NMR Spectroscopy. Carbon-13 MAS NMR spectra were obtained on a home-built Fourier transform NMR spectrometer, which consists of an Oxford Instruments (Osney Mead, U.K.) 11.7-T 2-in. bore superconducting solenoid magnet, a Nicolet (Madison, WI) Model 1280 computer system, and assorted digital and radiofrequency (rf) electronics. MAS NMR spectra were obtained by using a Doty Scientific (Columbia, SC) 5-mm MAS probe. For ^2H NMR, we used the 11.7-T spectrometer, as well as another home-built spectrometer, which consists of an Oxford Instruments 8.45-T 3.5-in. bore solenoid, a Nicolet Model 1180/2090-3C data system, and more assorted rf electronics. A home-built solenoid probe, 8-mm o.d. sample tubes, and 2.3-μs (90°) pulses were used for ^2H data acquisition (using the solid-echo technique).

Chemical Aspects. Monogalactosyl diglyceride [primarily 1,2-di[(9*Z*,12*Z*,15*Z*)-octadeca-9,12,15-trienoyl]-3-β-D-galactopyranosyl-*sn*-glycerol] and digalactosyl diglyceride [primarily 1,2-di[(9*Z*,12*Z*,15*Z*)-octadeca-9,12,15-trienoyl]-3-(α-D-galactopyranosyl-1–6-β-D-galactopyranosyl)-*sn*-glycerol] were both from Lipid Products, South Nutfield, U.K., and were used as received. Desipramine and imipramine were from Sigma-Aldrich Chemical Co. (St. Louis, MO). [2,4,6,8-$^2H_4$]Desipramine and [^2H_n]imipramine were synthesized bascially according to the protocol for imipramine as outlined by Tabeta et al. (1985). Imipramine differs from desipramine by the addition of a second *N*-methyl group on the aminopropyl side chain. ^2H incorporation was verified by ^2H and ^{13}C NMR and by field-ionization mass spectrometry, which gave the following isotopomeric compositions: for [2,4,6,8-$^2H_4$]desipramine, $^2H_1$, 0.8%; $^2H_2$, 7.2%; $^2H_3$, 35%; $^2H_4$, 54%; for [^2H_n]imipramine (5-min exchange), $^2H_1$, 26.9%; $^2H_2$, 4.8%; $^2H_3$, 1.1%; $^2H_4$, 1.0%. Samples for ^2H NMR were made up in ^2H-depleted H_2O (Aldrich).

Results and Discussion

We show in Figure 1 the 125.7-MHz (11.7-T) proton-coupled magic-angle sample-spinning (PC-MAS) NMR spectra of ca. 2:1 and 1:2 mole ratios of the tricyclic antidepressant drug desipramine–1,2-dimyristoyl-*sn*-glycero-3-phosphocholine (DMPC)–H_2O (50 wt % H_2O) at 40 °C. Both samples are very fluid, the lower desipramine-containing

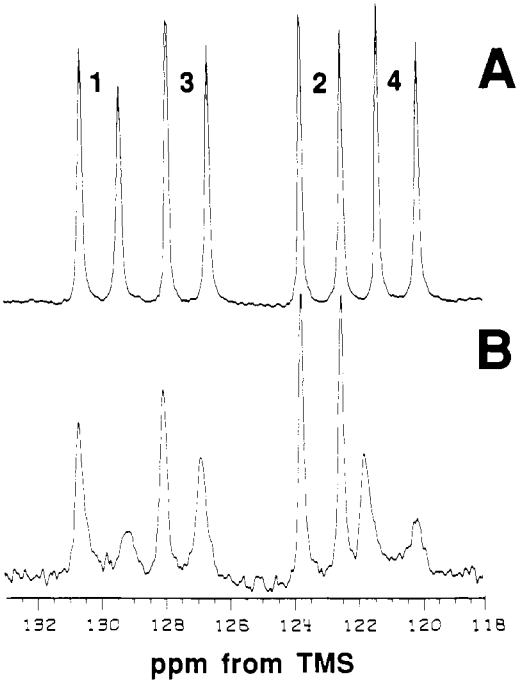

FIGURE 1: 125.7-MHz (11.7-T) proton-coupled ^{13}C MAS NMR spectra of DMPC–desipramine in H_2O (50 wt %). Only the protonated aromatic ring carbon doublet region is shown. The experimental conditions were (A) 68.8 mol % desipramine, 40 °C, 4-kHz MAS, 1500 scans, 5-s recycle time, 6.75-μs (90°) pulse width, and 7-Hz line broadening due to exponential multiplication and (B) 35.9 mol % desipramine and other conditions basically as in (A). The numbers above the doublets refer to the four different protonated aromatic carbons indicated in structure I.

sample being liquid crystalline, as determined by light microscopy, consistent with previous work (Cater et al., 1974). At high desipramine (I) concentrations, high-resolution ^1H

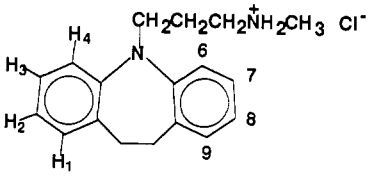

(I)

NMR spectra of both lipid and drug components are obtained even without MAS, so both components must undergo fast isotropic motions, and as expected the proton-coupled ^{13}C MAS NMR spectrum (Figure 1A) contains four sharp doublets, in the aromatic methine carbon region. However, in the lamellar phase, the C–H dipolar and ^{13}C chemical shielding interactions are not averaged to zero, and a far more complex spectrum is obtained. As can be seen from Figure 1B, each of the C–H doublets has a different line shape. The peaks for C2(8) and C3(7) are much less asymmetric than those of C1(9) and C4(6) [see Craik et al. (1987) for assignments], which we tentatively attribute to the C–H vectors of both C2(8) and C3(7) being close to the magic-angle—in this case the angle between the C–H vector and the C_2 axis of the molecule, assumed to be the director axis (Tabeta et al., 1985). In contrast, both C1(9) and C4(7) are essentially along this axis, so there is little averaging of the C–H dipolar interaction, due to motion about the C_2 axis. If the C–H dipolar interaction is averaged to $\sim$0 due to structural factors, then cross-correlation DLB effects will be small. This tentative assignment and explanation receive support from the observation of ^{13}C NMR line broadening of C1(9) and C4(7) of imipramine in *sonicated* vesicles under conditions of proton

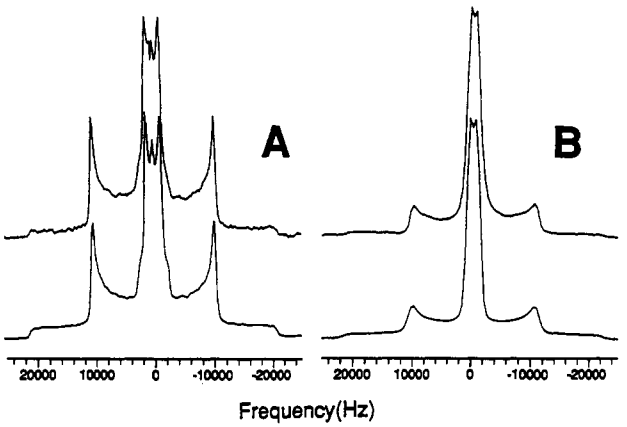

FIGURE 2: 55.7-MHz (8.45-T) ^2H spin-echo Fourier transform NMR spectra of [2,4,6,8-$^2H_4$]desipramine and [$^2H_{0.5}$]imipramine-1,2-dimyristoyl-*sn*-glycero-3-phosphocholine, in the presence of 50 wt % ^2H-depleted H_2O, at 36 °C. Spectral simulations are given on the bottom of the figure. (A) 30 mol % imipramine; (B) 30 mol % desipramine.

decoupling by Tabeta et al. (1985) and the ^2H NMR results shown in Figure 2. Here, we present 55.7-MHz ^2H NMR spectra, and line-shape simulations, for [$^2H_4$]desipramine and [$^2H_{0.5}$]imipramine–DMPC–H_2O. As can be seen from Figure 2, the ^2H NMR spectra both consist of two components, characterized by ^2H quadrupole splittings of ~0–2 and ~20 kHz. These experimental results are consistent with those of Tabeta et al. using [$^2H_4$]imipramine–egg lecithin, but our explanation is very different. Tabeta et al. assigned the sharp central peak to free imipramine, while their ~16-kHz component was assigned to H2(8), with H4(6) being invisible, due, it was thought, to its ~135-kHz quadrupole splitting.

We find no evidence for a very large quadrupole splitting (at any of the imipramine concentrations used by Tabeta et al.) using the spin-echo method and fast digitization (1 μs), even at long recycle times. In addition, the observation that the ~1:1 ratio between the ~0–2 and 20-kHz spectral components is independent of desipramine concentration (data not shown) strongly supports the idea that there is no 135-kHz component in either system. A more reasonable conclusion is, we believe, that the narrow (~0–2 kHz, quadrupole splitting) component arises from $^2H2(8)$, which is oriented approximately at the magic angle to the C_2 or director axis, and gives a very sharp doublet in the ^{13}C spectrum (Figure 1B). The 20-kHz component is then assigned to C–$^2H4(6)$, oriented approximately along the director axis, and this site gives rise to the very broad ^{13}C doublet at 121 ppm (Figure 1B). As may be seen from Figure 1B, the apparent *J*-couplings for C1(9) and C4(6) of ~184, 187 Hz are considerably larger than those of C3(7) and C2(8) of ~146, 155 Hz and are also much larger than those observed in the high desipramine phase (Figure 1A), where ^1J values of 155, 160, 160, and 157 Hz are obtained for C1(9), C3(7), C2(8), and C4(6). We belive these results indicate that each of the C–H splittings in Figure 1 has a scalar contribution of ~150 Hz, which cannot be removed by dynamical averaging. The splittings of the lines observed in Figure 1 arise, then, from a combination of scalar (*J*) and unaveraged dipolar and dipole–CSA interactions, and it is the *increase* in apparent splitting of ≈25 Hz that is much larger for C1(9) and C4(6) than for C3(7) and C2(8) (≈0 Hz), consistent with the ^2H NMR results.

Our results also give clear evidence for substantial reorientation of the desipramine 2-fold axis, since the largest quadrupole splittings (from $^2H1,4$) are only ~20 kHz, which is much less than the "rigid lattice" value of ≈135 kHz expected if the molecule reoriented *only* about the 2-fold axis.

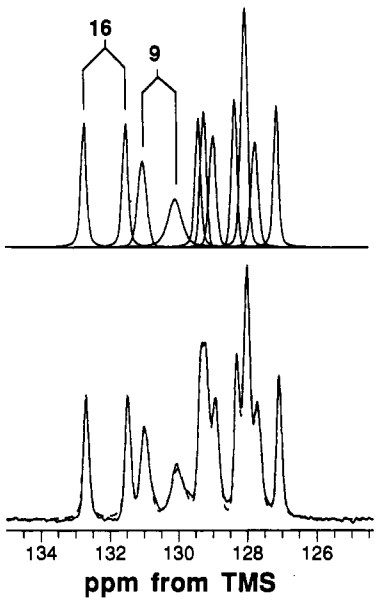

FIGURE 3: Unsaturated chain carbon region of the 125.7-MHz (11.7-T) proton-coupled ^{13}C MAS NMR spectrum of digalactosyl diglyceride–H_2O at 20 °C, together with (top) its computer line-shape simulation. Experimental conditions were 2.9-kHz MAS, 8237 scans, 5-s recycle time, 6.5-μs (90°) pulse width, and 7-Hz line broadening due to exponential multiplication. The dotted line superimposed on the experimental spectrum (below) is the composite simulated spectrum.

Support for the ^2H NMR assignments is given by the ^2H NMR result on [$^2H_{0.5}$]imipramine (Figure 2A). The two powder patterns are present in a 2:1 ratio (essentially independent of pulse spacing in the τ = 35–70-μs range), in complete agreement with solution ^{13}C NMR results (data not shown), which show ~0.18 ^2H at C2(8) and 0.36 ^2H at C4(6), also in agreement with the overall ^2H incorporation deduced from the mass spectral data.

We show in Figure 3 the 125.7-MHz (11.7-T) coupled ^{13}C MAS NMR spectrum of a 1:1 digalactosyl diglyceride (II)–water liquid-crystalline (L_α) multibilayer dispersion, in the olefinic carbon spectral region. There are two important features: (1) Both C9 and C10 (the first double bond) show DLB effects, suggesting a not-unreasonable increased order in the upper parts of the chain. (2) The DLB effect is much more pronounced for C9 than for C10, even though both are on the *same* double bond. An immediate explanation of this effect can be found in the work of Seelig and Waespe-Šarac̆evic̆ (1978) and Browning and Seelig (1980), who showed a magic-angle effect for the C(10)–^2H vector in several unsaturated lipids. As with desipramine and imipramine, fast internal motion of a C–H vector at or close to the magic angle collapses the C–H dipolar interaction and reduces any DLB.

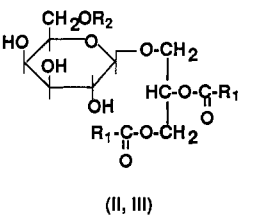

(II, III)

R_1= - $(CH_2)_7CH{=}CHCH_2CH{=}CHCH_2CH{=}CHCH_2CH_3$

II: R_2 = galactosyl; III: R_2 = H

Finally, we show in Figure 4 PC-MAS NMR spectra of monogalactosyl diglyceride (III) [primarily 1,2-di-[(9*Z*,12*Z*,15*Z*)-octadeca-9,12,15-trienoyl]-3-β-D-galacto-

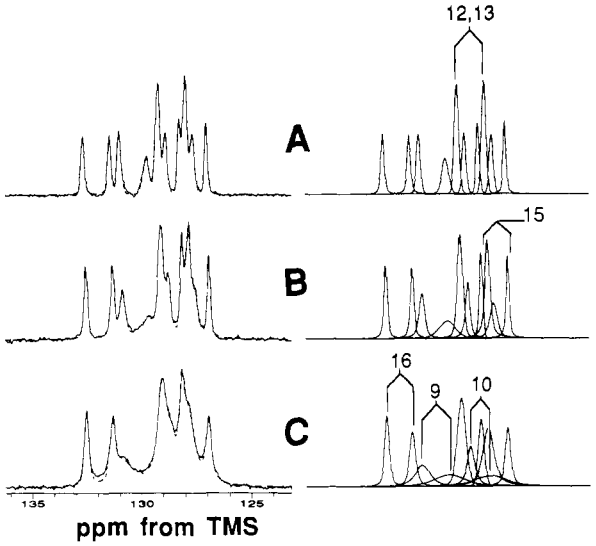

FIGURE 4: 125.7-MHz (11.7-T) proton-coupled ^{13}C MAS NMR spectra of monogalactosyl diglyceride–H_2O (50 wt % H_2O) at various temperatures, along with the simulated line shapes. Experimental conditions were (A) 20 °C, 2.9-kHz MAS, 2308 scans, 5-s recycle time, 6.5-μs (90°) pulse width, and 7-Hz line broadening due to exponential multiplication, (B) −20 °C, 3.0-kHz MAS, 1000 scans, and other conditions as in (A), and (C) −30 °C, 3.0-kHz MAS, 1128 scans, and other conditions as in (A). The numbers are the (*J*-coupled doublet) carbon peak designations.

pyranosyl-*sn*-glycerol]–H_2O (1:1 wt ratio), as a function of temperature, again in the olefinic carbon region. At 20 °C (Figure 4A), the spectrum is very similar to that of the digalactosyl diglyceride (Figure 3) and can be well simulated using 11 individual (1 two-carbon) peaks. As with the digalactosyl diglyceride, C9 and C10 show differential line-broadening effects, with the line widths for C9 being greater than for C10, again we believe due to a magic-angle effect at C10. On cooling to −20 and −30 °C (Figure 4B,C), all peaks broaden. Using a variety of constrained and unconstrained Levenberg–Marquart line-shape analyses, we have obtained simulations of the low-temperature spectra using the high-temperature (theoretical) intensity and (initial) chemical shift values. The results (Figure 4) show progressive broadening, as well as differential line broadening, as the temperature is lowered. C9/C10 is the first to broaden, followed by C12/C13; then at the lowest temperature investigated, DLB effects are seen in the computer simulations for each unsaturated carbon present, although the magic-angle orientation effect, i.e., a large difference in width between C_n and C_{n+1}, is restricted to $n = 9$ (where n is the carbon number of the atom in question).

Conclusions

The results we have presented above show the following interesting features: First, ^{13}C proton-coupled MAS NMR spectra of lipid–water systems can be readily obtained at high magnetic field strengths, and the *J*-coupled multiplets observed, more often than not, show large differential line-broadening effects. Second, such DLB effects are largest for aromatic rings or on olefinic double bonds. Third, magic-angle effects, in which the ^{13}C–H vector undergoes fast internal motion at an angle $\theta \sim \sec^{-1}\sqrt{3}$, where θ is the angle between the C–H vector and the axis of motional averaging, quench the DLB effect, as seen with C2(8) and C4(6) in desipramine and imipramine and with C10 in the mono- and digalactosyl diglycerides. Fourth, upon cooling, the mono- and digalactosyl diglyceride chains appear to become motionally restricted ("freeze" or "solidify") from the top of the chain downward. DLB effects for all six olefinic carbons are seen at low temperature in the monogalactosyl diglyceride–water system. Fifth, we have found interesting correlations between ^{13}C MAS DLB effects and results obtained by ^2H NMR. Related effects have also been observed in other liquid crystals, as well as in mobile polymers, e.g., poly(*cis*-isoprene) (Oldfield et al., 1991), and are not restricted to sp^2 carbons, since complex dipole–dipole (and higher order) cross-correlation effects are observed in many samples, e.g., the aliphatic carbon region of the desipramine–lecithin system (data not shown). For very congested spectral regions, two-dimensional methods such as those used by Lee and Griffin (1989) may provide useful resolution enhancements. When combined with variable-temperature coupled spin–spin and spin–lattice relaxation and field dependence studies, we believe that proton-coupled ^{13}C MAS NMR will become a very useful technique with which to investigate the structures of a wide range of mobile solids of chemical and biochemical interest, without use of sonication or isotopic labeling.

References

Browning, J. L., & Seelig, J. (1980) *Biochemistry 19*, 1262–1270.
Cater, B. R., Chapman, D., Hawes, S. M., & Saville, J. (1974) *Biochim. Biophys. Acta 363*, 54–69.
Craik, D. J., Hall, J. G., & Munro, S. L. A. (1987) *Chem. Pharm. Bull. 35*, 188–194.
Farrar, T. C., & Quintero-Arcaya, R. A. (1987) *J. Phys. Chem. 91*, 3224–3228.
Forbes, J., Bowers, J., Moran, L., Shan, X., Oldfield, E., & Moscarello, M. (1988) *J. Chem. Soc., Faraday Trans. 84*, 3821–3849.
Harris, R. K., Packer, K. J., & Thayer, A. M. (1985) *J. Magn. Reson. 62*, 284–297.
Hartzell, C. J., Stein, P. C., Lynch, T. J., Werbelow, L. G., & Earl, W. L. (1989) *J. Am. Chem. Soc. 111*, 5114–5119.
Lee, C. W. B., & Griffin, R. G. (1989) *Biophys. J. 55*, 355–358.
Mackor, E. L., & MacLean, C. (1966) *J. Chem. Phys. 44*, 64–69.
McConnell, H. M. (1956) *J. Chem. Phys. 25*, 709–711.
Oldfield, E., Chung, J., Le, H., Bowers, T., Patterson, J., & Turner, G. L. (1991) *J. Am. Chem. Soc.* (submitted).
Pines, A., Gibby, M. G., & Waugh, J. S. (1972) *J. Chem. Phys. 56*, 1776–1777.
Renou, J.-P., Giziewicz, J. B., Smith, I. C. P., & Jarrell, H. C. (1989) *Biochemistry 28*, 1804–1814.
Rothgeb, T. M., & Oldfield, E. (1981) *J. Biol. Chem. 256*, 6004–6009.
Seelig, J. (1977) *Q. Rev. Biophys. 10*, 353–418.
Seelig, J., & Waespe-Šarčevič, N. (1978) *Biochemistry 17*, 3310–3315.
Sefcik, M. D., Schaefer, J., Stejskal, E. O., McKay, R. A., Ellena, J. F., Dodd, S. W., & Brown, M. F. (1983) *Biochem. Biophys. Res. Commun. 114*, 1048–1055.
Shimizu, H. (1964) *J. Chem. Phys. 40*, 3357–3364.
Tabeta, R., Mahajan, S., Maeda, M., & Saito, H. (1985) *Chem. Pharm. Bull. 33*, 1793–1807.
Veksli, Z., Salsbury, N. J., & Chapman, D. (1969) *Biochim. Biophys. Acta 183*, 434–446.
Vist, M. R., & Davis, J. H. (1990) *Biochemistry 29*, 451–464.
Xu, Z.-C., & Cafiso, D. S. (1986) *Biophys. J. 49*, 779–783.